Analysis and Classification of EEG Signals

Author

MUNEEB ARSHAD

00000319157

Supervisor

DR. SHAHZAD AMIN SHEIKH

DEPARTMENT OF ELECTRICAL ENGINEERING

COLLEGE OF ELECTRICAL & MECHANICAL ENGINEERING

NATIONAL UNIVERSITY OF SCIENCES AND TECHNOLOGY

ISLAMABAD

December, 2021

Analysis and Classification of EEG Signals

Author

MUNEEB ARSHAD

00000319157

A thesis submitted in partial fulfillment of the requirements for the degree of

MS Electrical Engineering

Thesis Supervisor:

DR. SHAHZAD AMIN SHEIKH

Thesis Supervisor's Signature: _____

DEPARTMENT OF ELECTRICAL ENGINEERING

COLLEGE OF ELECTRICAL & MECHANICAL ENGINEERING

NATIONAL UNIVERSITY OF SCIENCES AND TECHNOLOGY,

ISLAMABAD

December, 2021

DECLARATION

I certify that this research work titled "*Analysis and Classification of EEG Signals"* is my own work. The work has not been presented elsewhere for assessment. The material that has been used from other sources it has been properly acknowledged / referred.

Signature of Student
MUNEEB ARSHAD
00000319157

LANGUAGE CORRECTNESS CERTIFICATE

This thesis has been read by an English expert and is free of typing, syntax, semantic, grammatical and spelling mistakes. Thesis is also according to the format given by the university.

Signature of Student

MUNEEB ARSHAD

00000319157

Signature of Supervisor

COPYRIGHT STATEMENT

ACKNOWLEDGEMENTS

I thank The Almighty Allah for enabling me to complete this thesis. This thesis would never have achieved fruition without the moral and financial support of my parents, who have supported me. I also want to thank my supervisor Dr. Shahzad Amin Sheikh and GEC Members Mr. Kamran Aziz Bhatti and Dr. Fahad Mumtaz Malik for their guidance and support.

I dedicate this thesis to

My Supervisor and GEC Members

ABSTRACT

Objective. The classification and features extraction is extremely important part of brain computer interface (BCI) systems. During the previous few years, deep learning techniques have been employed on different types of data for features extractions, and classification purposes. However, few people have employed these deep learning techniques on BCI applications. ***Approach*** The goal is to acquire features using the deep learning techniques, which eventually enhance the model classification performance. In this research, we investigated at the integration of CNN and LSTM. The proposed CNN architecture comprises of four block for the purpose of features extraction. Each block comprises of a Convolutional Layer, Batch Normalization Layer (BNL), Rectified Linear Unit (RELU) activation layer and one Max-Pooling layer. To begin, we converted motor imagery EEG signals into 2D images using the Continuous wavelet transform. These images are fed in to a proposed framework. CNN Block are used to extract robust features and LSTM architecture for classification purposes. ***Main results.*** Our model was assessed on the dataset III of BCI competition II where we achieved 96.43% and kappa value reached 0.9286. We also assessed the performance of our suggested model on Dataset 2b from BCI Competition IV where it achieved average accuracy of 86.83% and average kappa value of 0.742.

Significance. Our proposed method has shown that deep learning technique gave remarkable classification results compared to traditional approaches.

Keywords: BCI, Motor imagery, CNN, LSTM

TABLE OF CONTENTS

LIST OF FIGURES

LIST OF TABLES

ACRONYMS

AAR	Adaptive Auto-Regressive
BCI	Brain Computer Interface
CNN	Convolutional Neural Network
CSP	Common Spatial Pattern
DBN	Deep Belief Network
EEG	Electroencephalography
ERD	Event-Related Desynchronization
ERS	Event-Related Synchronization
FAWT	Flexible Analytic Wavelet Transform
LDA	Linear Discriminant Analysis
MI	Motor Imagery
ReLU	Rectified Linear Unit
SSVEP	Steady State Visual Evoked Potentials
STFT	Short Time Fourier Transform

CHAPTER 1: INTRODUCTION

1.1 Background, Scope and Motivation

The advancement of computing and deep learning has led to a revolution in our lives. Since 1970s, engineers have made remarkable progress to fill the communication gap between computer technology and humans. The computational Intelligence has further remove the communication barrier between computer technology and humans [1]. Today, the BCI serves as a medium between the human brain and the outside world. BCI systems are classified into two types.: 1) invasive and 2) non-invasive.

Non-invasive brain computer interfaces (BCIs) have measuring sensors placed outside the head, such as on the scalp. Invasive brain computer interfaces (BCIs) are those in which electrodes are surgically implanted into the brain. Electroencephalography (EEG) equipment is normally employed in the BCI System to acquire brain signals as it has a high time resolution, non-invasive characteristic [2].

For healthy and unhealthy people, BCI systems have been researched for range of purposes. Modeling a comprehensive BCI system especially for commercial use remains a difficult task. As control signals in BCI, different types of brain signals have been used. MIs, SSVEPs and P300 evoked potentials are the most prevalent signals. The activity state of the brain is examined in the case of a MI by imagining limb motions. Signal processing and artificial intelligence techniques are used in BCI systems to comprehend these brain activities. As a result, computational modeling and signal processing tools have a massive influence on BCI effectiveness. Traditional classification methods have proven to be effective in a variety of contexts. Deep learning algorithms, on the other hand, have been successfully used to solve machine learning challenges, particularly in image processing, audio recognition, and natural

language processing. For image classification, deep learning techniques are particularly helpful in detecting complicated features and patterns. Deep neural networks are capable of modelling both complex features and non-linear interactions between them. These facts forced us to utilize deep learning techniques to classify EEG signals.

Through a series of studies in which MI is used as BCI control signal and Neural Networks are employed for recognition or classification, we investigate the EEG data acquisition, processing, and feedback phases in BCI. The goal of this research is to explore into brain-computer interface devices that employ EEG to acquire signals. This study's main purpose is to investigate the signal processing element of BCI. In this study, motor imagery signals are exploited to control the BCI system. The use of deep learning approaches to classify MI-related brain signals is being researched. Through a series of studies, this thesis investigates the acquisition, processing, and feedback of EEG signals in BCI, using deep learning algorithms for feature extraction and classification.

1.2 Literature Review

In this study, we employed Motor Imagery (MI) Signals as control signals, which determine the activity state of brain by using the imagination of limb movements. For example, when a person imagines the unilateral movement, the phenomena ERD and ERS occurs [3,4].

EEG signals are typically processed in five steps. 1) signal acquisition, 2) pre-processing, 3) feature extraction, 4) classification and 5) control as illustrated in Figure 1-1. EEG signals usually processed in five steps 1) signal acquisition, 2) pre-processing, 3) feature extraction, 4) classification and 5) control as illustrated in Figure1. Now a day’s, researchers are working on features extraction algorithms. Different approaches are used to extract features, such that, AAR, CSP, Short Time Fourier Transform (STFT), Wavelet Transform (WT) etc.

Conventional Features extraction techniques are relatively matured, but some problems still exist in them. For example, in the above stated models, the Adaptive Auto Regressive (AAR) model is more appropriate for inspecting the stationary signals. Most researcher used wavelet transform to extract statistical features as EEG features. But this approach is not robust because motor imagery signal pattern is random in nature and causes uncertainty due to trails and individuals. In case of STFT, the size of window defines the frequency resolution and time resolution, e.g. if window size is narrower, a better time resolution will obtain and frequency resolution will become worse. Contrary, if the window is wider, a better frequency resolution will obtain and time resolution will become worse. In STFT, the frequency resolution and time resolution cannot be attained concurrently. Narrow window causes a spectrum leakage which is another main problem in STFT.

Deep learning techniques have been successfully deployed in recent years and enhanced in image processing, speech enhancement, and natural language processing. [5-7]. The significance of a deep network is that it can automatically extract features, avoiding the drawbacks of manually extracting features. In [8], the CSP technique was used to get features and a four-layer based neural network was built to identify Motor Imagery EEG signals. After performing the experiments, we get to know that the features extracted by CSP helped to reduce the amount of calculation.

In [9] Deep Belief Network (DBN) and an implicit Markov model (HMM) were employed to detect emotions by utilizing the differential entropy of signals in five frequency bands and their sum in the EEG signal as a feature. The accuracy of classification model was greater when compared to a classic SVM and a KNN models. In [10], the features were extracted using the FAWT and the LDA was used for classification. In [11], wavelets transformation was employed on EEG Signals to extract features and Two-Layer CNN was used for classification

purpose. When compared to the DDFSB and RQNN models, the classification accuracy and kappa value were higher.

Although the aforementioned models used deep neural networks for classification, the features were still extracted manually as input. Manual feature extraction approaches have limitations and unable to extract appropriate features well, resulting in low classification accuracy [12]. However, Deep Neural Network can learn more abstract features than traditional Machine Learning because of its not linear characteristics and can improve classification accuracy.

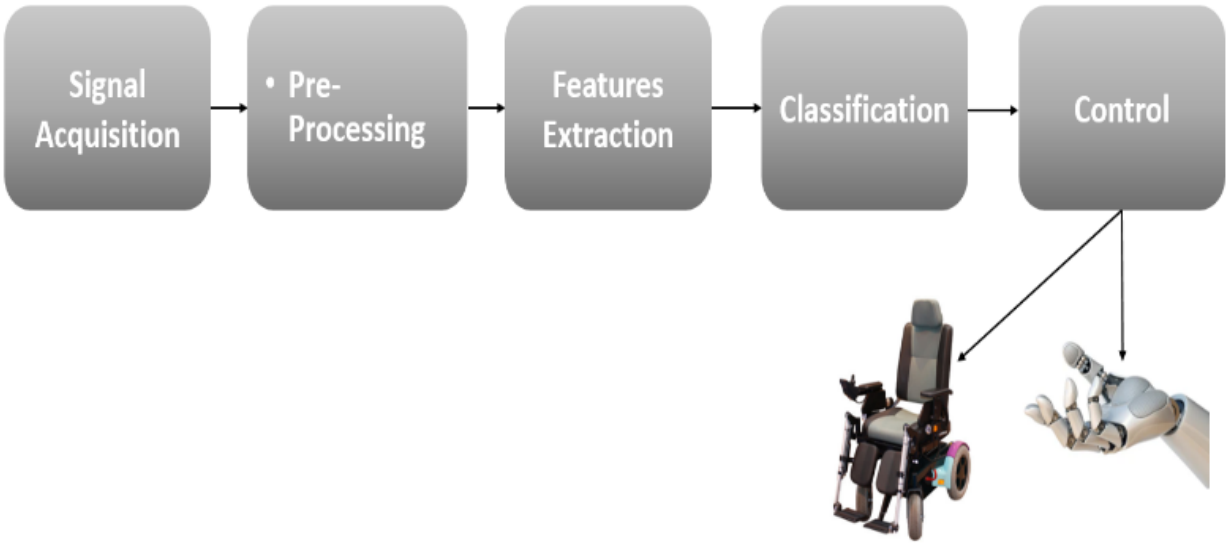

Figure 1-2: Motor Imagery EEG Based System.

1.3 Thesis Outline

Chapter 2: A brief overview of Brain Computer Interface Systems is discussed in this chapter. This chapter also provide insight knowledge of data acquisition, synchronous and asynchronous BCI and Neurological phenomena. etc.

Chapter 3: This chapter provide in depth knowledge of our Proposed Methodology.

Chapter 4: This chapter provide information regarding Dataset and Results.

Chapter 5: This chapter contains conclusion.

CHAPTER 2: BRAIN COMPUTER INTERFACE SYSTEMS

The brain communicates with the peripheral nervous system, which governs the body. This process starts with an intention of a person and pass through the peripheral nerves till it reaches the desired bodily component. Recently, there is a lot of growth in the technology that records the electrophysiological signals, which have created potential approaches for bypassing the peripheral nervous system, ultimately controlling a device directly from the brain. A "brain computer interface" is a system that converts neural activity into device control commands. (BCI) [13].

A Brain-Computer Interface (BCI) is a device that measure the patterns form the activity of brain. These patterns are generated when the user have an intent, which then uses for communication and the purpose of control. For people with motor limitations, this can be extremely beneficial. BCI, on the other hand, isn't just for persons with impairments. It can also be used for various applications e.g. controlling a wheelchair.

This chapter aims to deliver the overall view of the various components of a BCI system. We talked about brain structure in part 2.1. Part 2.2 explains how brain data acquisition is used in BCI, and Part 2.3 compares asynchronous and synchronous BCI systems. Neurological phenomena are briefly explained in part 2.4, EEG signal processing in part 2.5, and BCI system applications in part 2.6.

2.1 Brain Structure

The brain stem, cerebellum, and cerebrum are the three components of the human brain. The cerebrum is categorized in two hemispheres: left and right. The outer layer of the cerebrum is known as cortex. It contains four zones termed as "lobes." as shown in Fig.2-1.

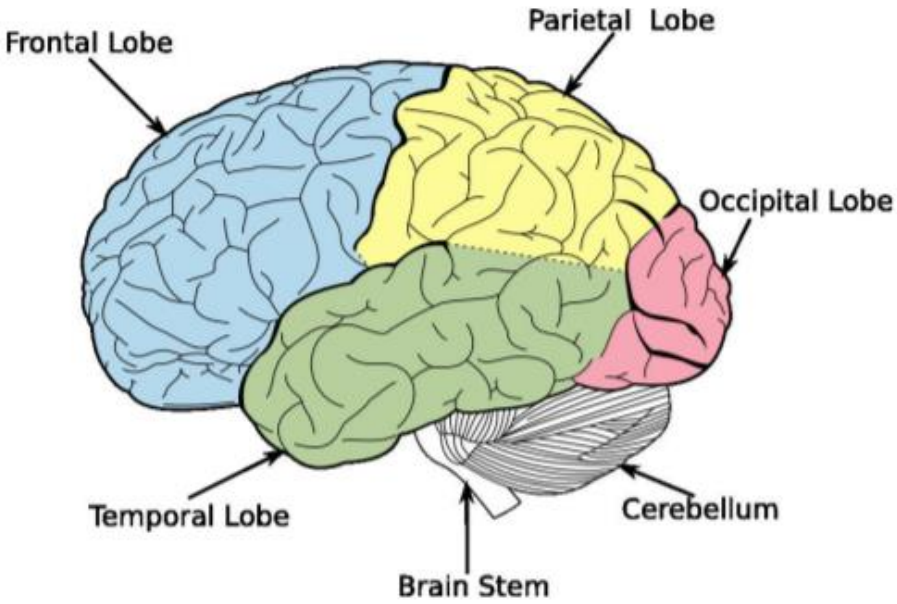

Figure 2-1 Lateral view[14]

The frontal lobe is in charge of cognitive abilities such as speech, movement, and executive functions. Auditory, visual, and language functions are all handled by the temporal lobe. It's also utilized to deal with emotions. Reading/writing, language comprehension, attentiveness, and spatial awareness are all functions of the parietal lobe. Finally, the occipital lobe aids visual processing. [14].

2.2 Acquisition of Brain Data

Electroencephalogram (EEG) signals are the electrical fields, which are produced by the neurons. Electrodes receive these fields and emit a signal with a low amplitude. The EEG

electrodes are usually linked to a cap and put on the surface of the head. Gel or salty water is used to improve the conductivity between the skull and the electrodes. This means that any EEG system will take a certain amount of time to set up (typically 20 minutes). The 10-20 system is often used to put electrodes as shown in Figure 2-2.

Rhythms are oscillations in the brain that can be seen in certain areas and at specific frequency bands. They have the ability to convey the data of the mental state of a person, which can be manipulated willingly. These rhythms are known as alpha, beta, gamma, delta, theta, and mu. It is illustrated in Figure 2-3.

Alpha rhythm(8-13Hz): The alpha rhythm is found in the posterior (occipital) region of the brain, with a higher frequency on the non-dominant side. It is most noticeable when one closes their eyes or is in a calm mood.

Gamma rhythm (more than 30Hz): Although scalp-based EEG is difficult to detect, the gamma rhythm is related to cognitive and motor activity.

Delta Rhythm(1-4Hz): In humans, the delta rhythm is frequently found during the deep sleep.

Theta rhythm (4-8Hz): Theta rhythm can be detected while a young child in a state of drowsiness, when a user is attempting to suppress a response or action. It is also known to cause a spike when the user attempts to suppress a response or action. [15].

Mu rhythm (8-13Hz): The mu rhythm is a motor-based rhythm that changes as the user moves [16].

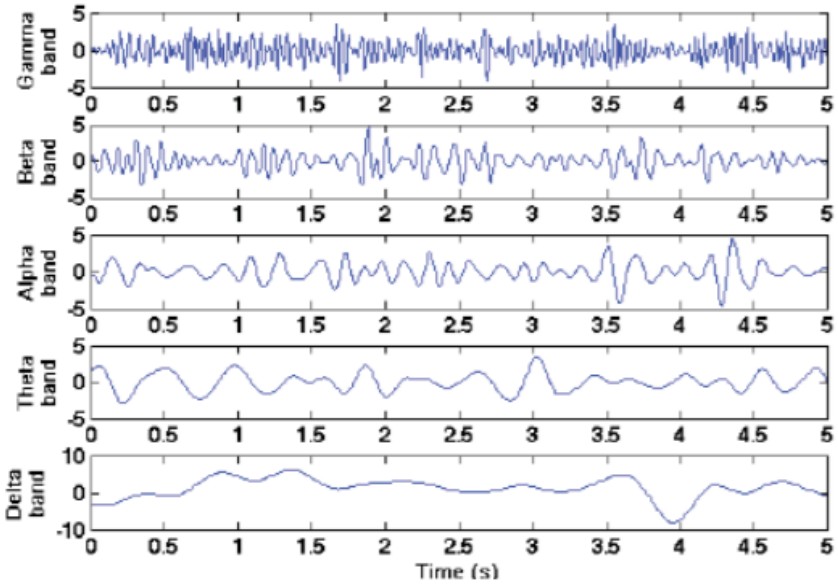

Figure 2-2: Different EEG Rhythms [17]

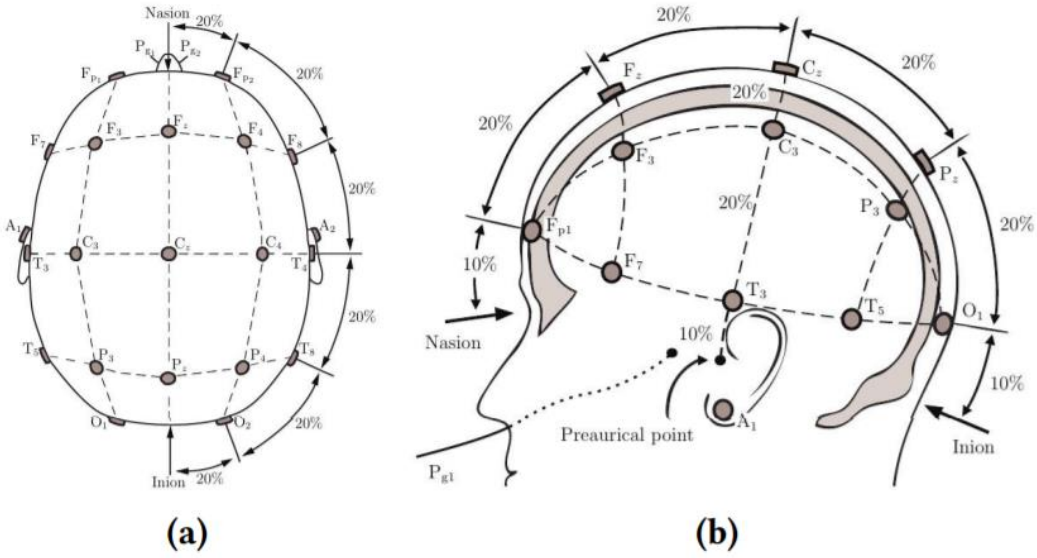

Figure 2-3: The international electrode placement system 10-20 [18] (a) Axial view. (b) side view

2.3 Synchronous vs Asynchronous BCI

A brain-computer interface can operate in two modes: synchronous mode and asynchronous mode [19].

In a synchronous mode of BCI, a prompt cue is displayed to the user on a regular basis. In order to control the device, the subject can develop mental states while the cue is on the screen.

In an asynchronous BCI, no indications are displayed, and the user can develop mental states aimed at controlling the device at any time. [20]

2.4 Neurological phenomena

The brain may generate various brain activity signals due to the causes of conscious or unconscious. The majority of these signals are yet unknown. On the other hand, the physiological phenomena, of some of these signals, are well recognized that were used in the applications of BCI. These signals include P300 evoked potentials, Steady State Visual Evoked Potentials (SSVEPs), Slow Cortical Potentials (SCPs), Sensory-Motor Rhythms, and Motor Imagery. [21]

2.4.1. SSVEP

When a person glances at something that flickers at a given frequency, his or her EEG signal can be identified with that frequency (and its upper harmonics). This paradigm is followed by a BCI that shows multiple items flickering at different frequencies and analyses the frequency peaks in the user's EEG to determine which object the user is gazing at right now [22].

2.4.2. Slow cortical potentials (SCP)

Humans can attempt to govern these potentials for both positive and bad effects. When the EEG signal levels are below/above a baseline level for 300 ms to several seconds, a negative/positive shift occurs. A user is given feedback information reflecting the current

average value of the EEG signal in a SCP-based BCI. A handler seeks to elicit a positive or negative potential change while focusing on this feedback data [23]

2.4.3. P300

The P300 event is defined as a 300 millisecond surge in the peak value of the EEG signal after the subject has been anticipating a stimulus. After providing a prominent stimulus in the middle of a series of not prominent stimuli, the P300 potential occurs.

The P300 speller is a BCI that is based on the P300 paradigm. A P300 speller application displays a matrix of letters to the user, which highlights one row or column at random in the matrix. The algorithm's goal is to determine which column and row the P300 potential occurs in, and thus which letter the user is looking for [24].A sample character is shown in Figure 2-4.

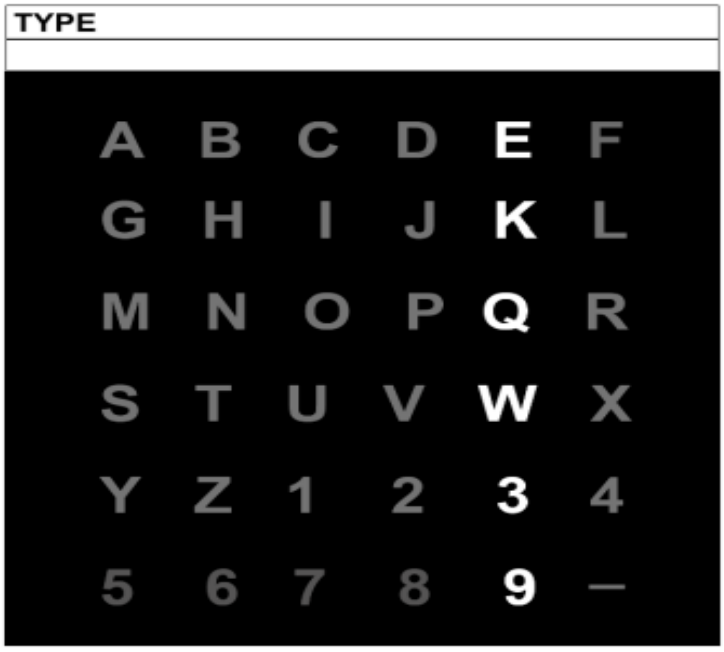

Figure 2-4: P300 spelling paradigm character matrix [25]

2.4.4. Event-related desynchronization (ERD) / Event-related synchronization (ERS)

The ERD/ERS phenomenon related with motor imagery acts has different spatial features and strength for different limbs, with the contralateral hemisphere being stronger and the ipsilateral hemisphere being weaker. The contralateral hemisphere is located on the side of the body opposite the limb for which the motor imagery task is performed, whereas the ipsilateral hemisphere is located on the same side of the body. The left hemisphere feels ERD/ERS when a person imagines a movement with his or her right hand [26]. The process is illustrated in Figure 2-5, Figure 2-9

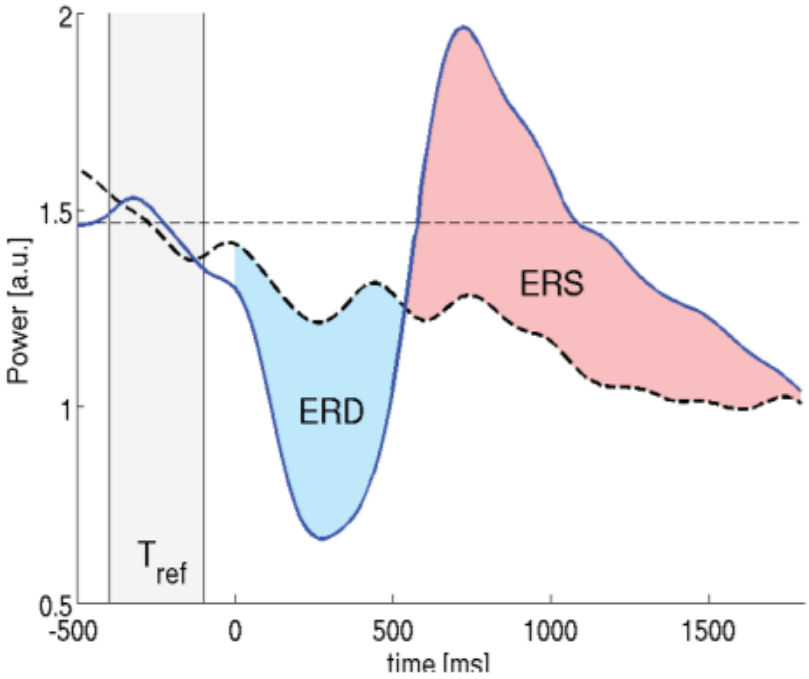

Figure 2-5: ERS and ERD during task [27]

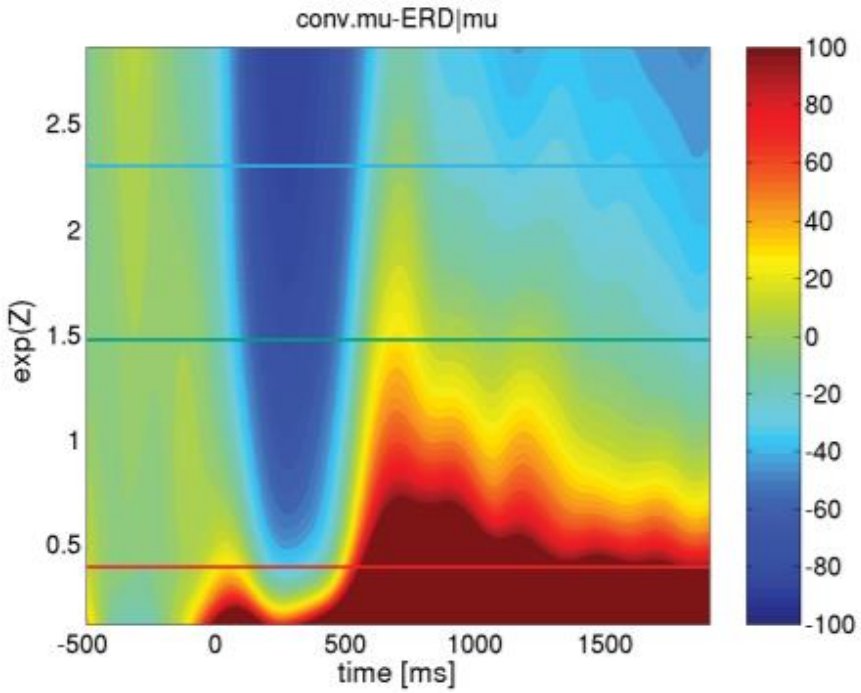

Figure 2-6: ERS and ERD during task [27]

2.5 EEG Signal Processing

The primary components of EEG Signal Processing are as follows:

Preprocessing: An EEG channel's recorded data contain a variety of undesirable sources, including artifacts, brain signals, and noise. As a result, the gathered signals are filtered in this step to extract appropriate signal frequency contents.

Feature Extraction: This is a crucial phase that aims to extract particular and useful data from the EEG recording. There are different methods to extracts features. The common approaches used to extract features are common spatial pattern (CSP), Adaptive Auto Regressive (AAR), Short Time Fourier Transform (STFT), Wavelet Transform (WT) etc.

Signal classification: The Selection for a model, which is compatible with the feature vectors, is the first step in the classification process. After choosing the best classifier model, the suitable parameters of the proposed model are found, and its prediction accuracy is improved

by using the training data. Following that, the training model will be verified, and the model gets will be tested on a test set to determine how well it performs in practice. The bias-variance trade-off problem has long been a source of concern for classifiers [28]. If we consider the simplicity or complicity, the classification model may not be effectively matched to the goal, resulting in low-performance classifiers. ***Under fitting*** occurs when a model or algorithm fails to effectively fit the data, that is, when the model has low variance but high bias, particularly if the model is extremely basic. When a statistical model encapsulates data noise, overfitting will occur. ***Overfitting*** happens when a model or algorithm fits the data too well. This is often the result of an overly sophisticated model with low bias but high variance**.** It is illustrated in Figure 2-6.

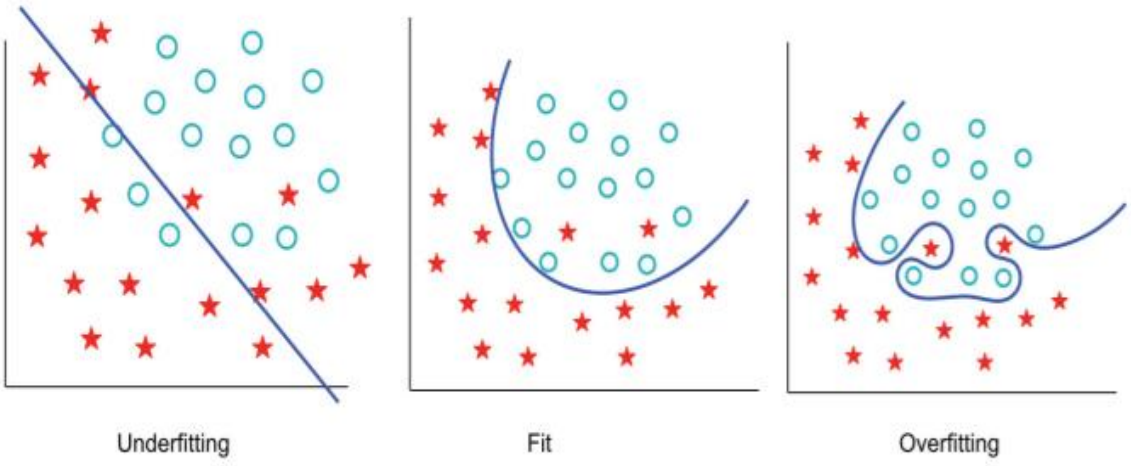

Figure 2-7: The bias-variance trade-off problem, i.e., problem of under fitting and overfitting

2.6 BCI Applications

BCI has many applications as it produces new channels for communication and control without using the peripheral nerves and the muscles. As a result, people with motor difficulties may find it extremely beneficial. People who have significant communication issues are among the primary beneficiaries of BCI. People with motor limitations can also use BCI to manage their surroundings.

Any BCI system will use various types of feedback signals to interact with the user. These feedbacks enable the user to adapt to the system as well as the system to the user. Using the BCI system's online feedback signals, subjects learn to control their brain processes. Using the collected data, Artificial Intelligence methods could be used to train the BCI system [29].

People, that have motor disabilities, BCI helps them to control their surroundings. It includes controlling the wheelchairs, room temperature and light that can make a difference in these people's lives [30]. Another BCI application that assists impaired individuals with transportation is Locomotion. Speech communication is among the most common applications of the BCI for those with communication impairments. There has been numerous research in this area. A range of brain activity were used in these research to choose the target letter from an on-screen display. The extensively utilized paradigms for BCI control in communication applications is P300 event-related brain potentials. Many speech communication research in BCI [31-35] employ these signals. Stable state visual evoked potentials(SSVEP) are another sort of control signal that has been employed for voice communication [36-40].

CHAPTER 3: METHODOLOGY

BCI is used to categorizes each brain activity pattern based on its characteristics. As a result, filtering is critical to the performance of BCI systems. This chapter describes the signal processing strategies employed in this study. In addition, this section provides an overview of the feature extraction and classification methods used in this study.

3.1 Signal Pre-Processing

The primary objective of signal preprocessing is to discard noise from the signal and to remove unwanted frequency components. Low-frequency noise can be found in some signals, causing problems with signal interpretation [41]. So preprocessing is needed to eradicate the baseline of the signals. The predominant acquisition channels for MI EEG signals are C3, Cz, and C4. We considered signals only from C3 and C4 channels. The purpose of using C3 and C4 channels is to reduce input signal redundancy and noise [42]. The first step in pre-processing is to remove the signal's superfluous frequency component. To achieve our desired frequency band, we constructed a band-pass filter with a range of 8–30 Hz.

3.2 Wavelet Transformation

When it comes to extracting valuable features from a signal, different people have different evaluation standards. STFT is also used for time frequency representation, but the problem with STFT is that neither the time resolution nor the frequency resolution can be obtained concurrently. The frequency resolution and time resolution are defined by the transform; for example, if the window is narrower, the time resolution will improve while the frequency resolution will deteriorate, and vice versa. To overcome the time-frequency resolution issues a continuous wavelet transform is used in this study. After applying CWT on EEG Signals we

get 2D images. In terms of time and frequency, the wavelet transform is a good tool for evaluating non-stationary signals. The calculation formulas of Continuous wavelet are represented as

$$W(a,\tau) = \frac{1}{\sqrt{a}} \int_{-\infty}^{\infty} x(t)\varphi(\frac{t-\tau}{a})dt \quad (1)$$

$$\varphi(x) = e^{-x^2} \cos(\pi \sqrt{\frac{2}{ln2}}\, x) \quad (2)$$

where x(t) represent signal sequence, the factor τ controls the wavelet function's translation, which corresponds to the signal's time domain information. $\varphi(x)$ is the mother wavelet.

Three electrode recordings were included in the datasets used in this study (C3, Cz and C4). These electrodes were implanted on the motor cortex of the brain, as shown in Figure 3 1.

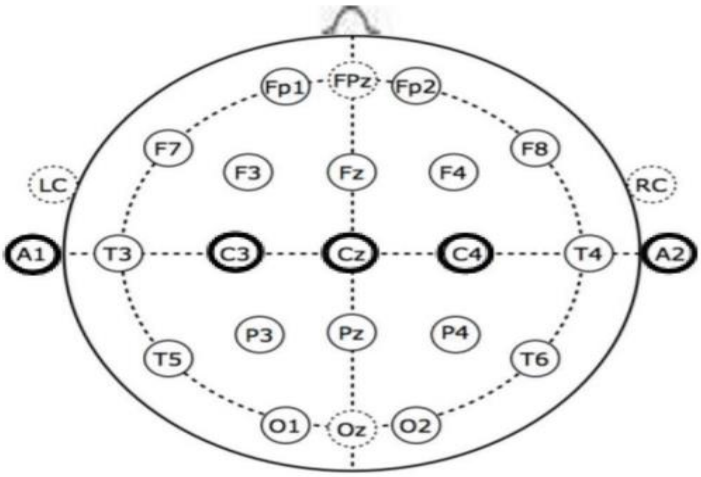

Figure 3-1: Positions of Electrodes in the 10-20 distribution

In the cerebral cortex ERD/ERS events occur. As the person executes imagery movement, the mu and beta rhythms energy changes. The energy in the relevant frequency band of the cerebral

cortex at the C3 electrode location increases when the individual performs left-hand motor imagery, while the energy in the corresponding frequency band of the cerebral cortex at the C4 electrode location declines. When a person performs right hand motor imagery, the energy in the relevant frequency band of the cerebral cortex at the C4 electrode location increases, while the energy in the relevant frequency band of the cerebral cortex at the C3 electrode location decreases [42]. Figure 3-2 shows an example of each of these.

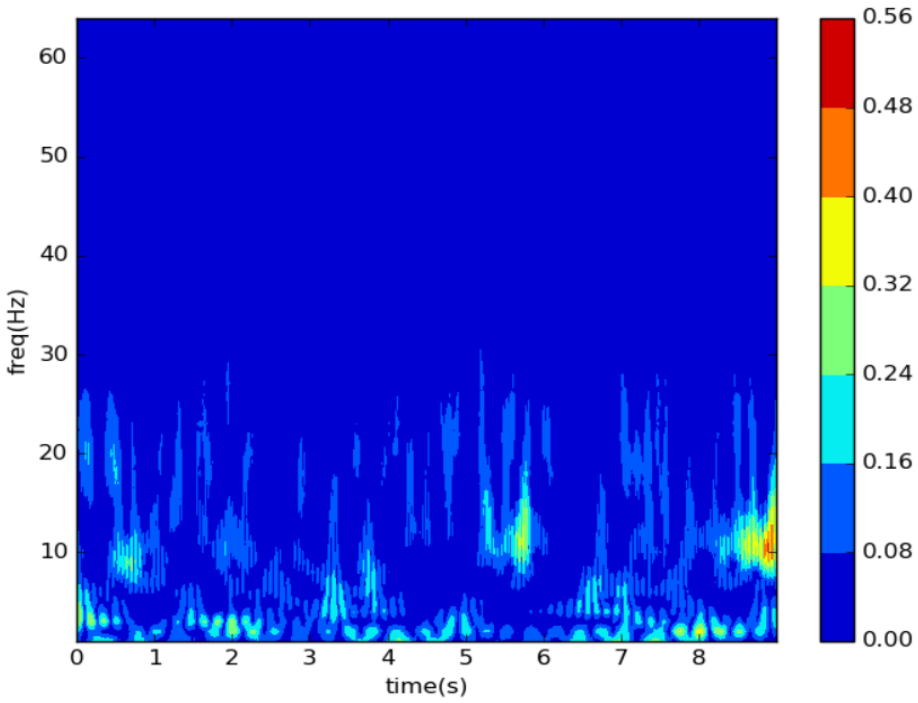

(a)

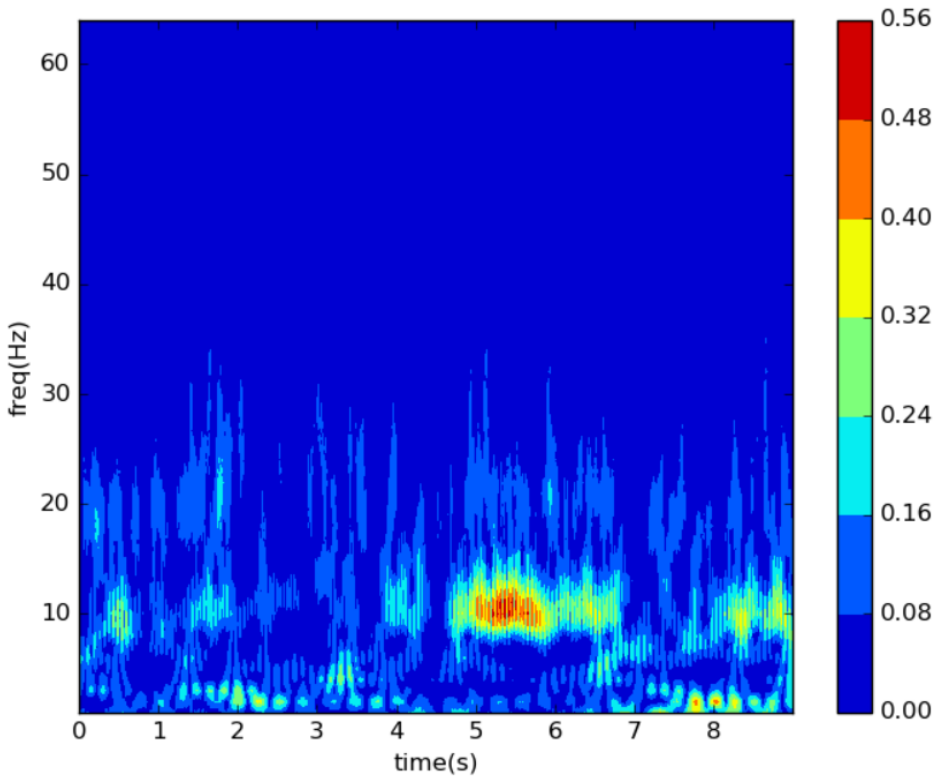

(b)

Figure 3-3: (a) Time frequency image of C3. (b) Time frequency image of C4. ERD/ERS phenomenon occur.

The Cz channel was excluded since it does not increase accuracy and instead introduces noise [42]. so C3 and C4 channel are appropriate for classification. Figure 3-4 depicts an image containing the C3 and C4 channels..

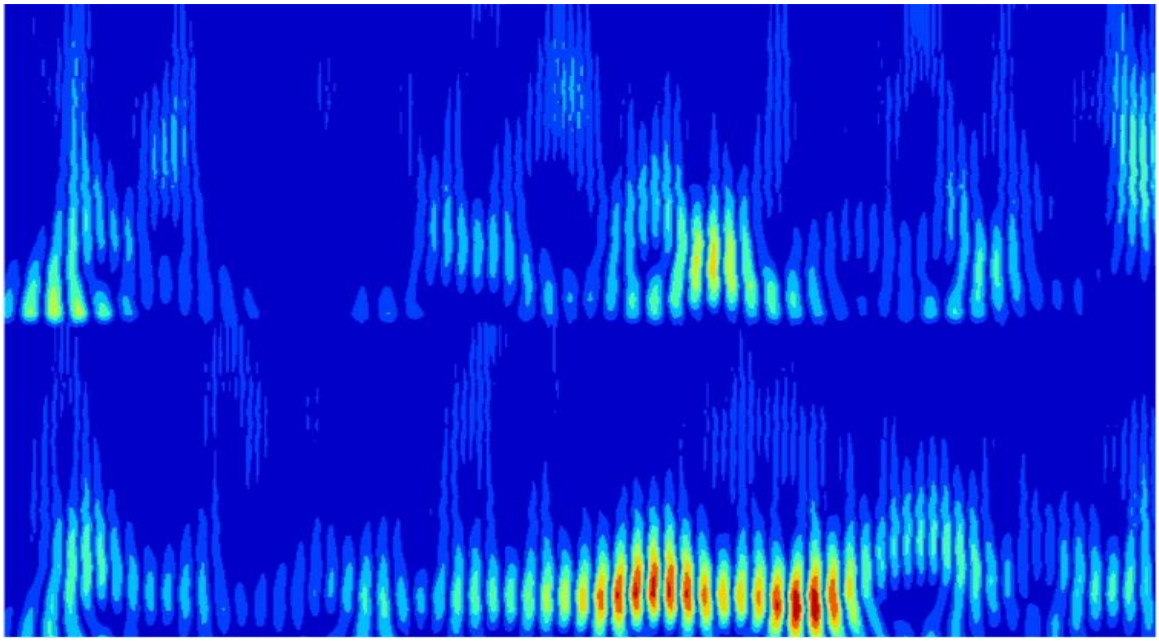

Figure 3-5: Image containing C3 and C4 channel

3.3 Convolutional Neural Network Framework

The original EEG signals are transformed into a two-dimensional images by using the wavelet transform. Following that, 2D images are embedded in a CNN. CNN Architecture is comprised of three blocks. One convolutional layer, one batch normalization (BN) layer, one rectified exponential linear unit (RELU) layer, and one max-pooling layer are included in each block. The feature learning block's core layers are the convolution and pooling layers [43]. The convolution layer's most significant qualities are spatially local connection and shared weights. [43–47]. In order to extract features from the input images, they are processed using a convolution layer. A kernel is used to convolve the image. A kernel is a tiny matrix with dimensions lower than the image to be convolved. This kernel slides across the image input's height and breadth and produced feature map using dot product.

The signal x(i,j) is incorporated into the 2D convolution layer, and then signal x(i,j) convolves with the kernel w(i,j) of size m x n. The equations are represented as

$$y(i,j) = x(i,j) * w(i,j) \quad (3)$$

$$y(i,j) = \sum_{l=-s}^{s} \sum_{m=-t}^{t} x(l,m).w(i-l,j-m) \quad (4)$$

The convolved features are subsequently placed in the BN layer, which at each batch normalizes the activations of the preceding layer. The BN layer boosts deep network efficiency and stability.

When the normalized features are embedded into the Rectified Linear Unit (ReLU) layer. ReLU layer takes any real value but only activate when the input is greater than zero. The equation is represented as

$$R(u) = \max(0,u) \quad (5)$$

The output features are embedded in to Pooling Layer. Using pooling layers, the dimensions of the feature maps are decreased. As a result, the number of parameters and processing time are both reduced. Using max pooling, the maximum element from the region of the feature map covered by the filter is chosen. The max-pooling layer's output will be a feature map that contains the most significant feature from the previous feature map.

3.4 Long Short Term Memory

RNNs (recurrent neural networks) are a sort of neural network that can be used to model sequential data [48]. Short-term dependencies can be learned from traditional RNNs, but due to exploding and vanishing gradients RNN failed to extract long term dependencies. LSTM is a form of RNN that handles with exploding and vanishing gradients. [49]. It is capable of extracting both short-term and long-term dependencies.

An LSTM is comprised of four components: an input gate, an output gate, a forget gate, and a cell. The LSTM can change the block state by removing or adding information. The following are the LSTM input outputs and corresponding equations for a single time step. [50-52]

$$\boldsymbol{f_t = \sigma_g(W_f \times x_t + U_f \times h_{t-1} + b_f)} \quad (6)$$

$$\boldsymbol{i_t = \sigma_g(W_f \times x_t + U_i \times h_{t-1} + b_i)} \quad (7)$$

$$\boldsymbol{o_t = \sigma_g(W_o \times x_t + U_o \times h_{t-1} + b_o)} \quad (8)$$

$$\boldsymbol{c'_t = \sigma_c(W_c \times x_t + U_c \times h_{t-1} + b_c)} \quad (9)$$

$$\boldsymbol{c_t = f_t . c_{t-1} + i_t . c'_t)} \quad (10)$$

$$\boldsymbol{h_t = o_t . \sigma_c(c_t)} \quad (11)$$

$\boldsymbol{\sigma_c}$: **tanh** $\boldsymbol{\sigma_g}$: **sigmoid**

$\boldsymbol{f_t}$ ***is the forget gate***

$\boldsymbol{i_t}$ ***is the input gate***

$\boldsymbol{o_t}$ ***is the output gate***

$\boldsymbol{c_t}$ ***is the cell state***

$\boldsymbol{h_t}$ ***is the hidden sate***

3.5 Combined CNN+ LSTM

This framework is built to learn features as well as classify them. The framework is comprised of four distinct feature learning blocks. Each block has two-dimensional convolution and pooling kernels. The convolution kernel has a size of 2x2, the stride has a size of 1x1, and the padding is the same. The first and second FLBs each have 64 convolution filters, while the third and fourth FLBs each have 128 convolution filters. The kernel size and max-pooling stride in the FLB are both 2x2, whereas the size in the other blocks is 4x4. This architecture's top layer contains a softmax classifier.

After that the acquired features are then fed in to LSTM layers, which extract additional temporal features. Following that, the output features are routed through a succession of fully connected layers, with the softmax layer acting as a classification layer. Figure 3-4 depicts the block diagram of our proposed technique.

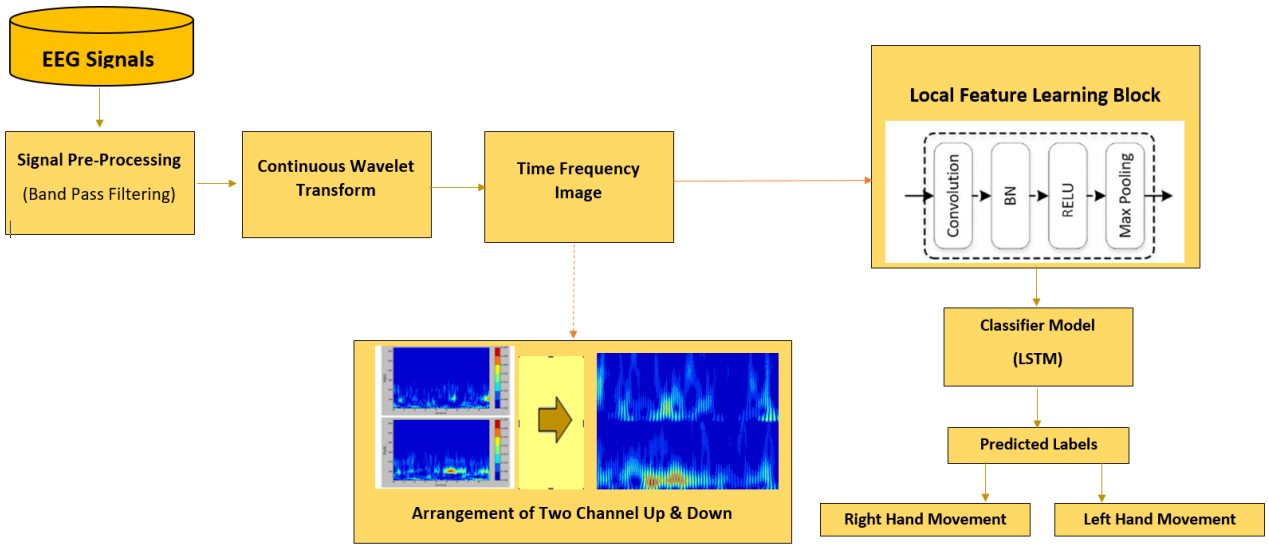

Figure 3-4: Proposed Method

CHAPTER 4: DATASET AND RESULTS

4.1 Dataset

We used two datasets to evaluate the efficiency of our architecture: The first dataset is taken from dataset III from BCI Competition II [53] and the second dataset is taken from BCI Competition IV dataset 2b [54] . The sampling rate of 128 Hz was used to record the dataset III from BCI Competition II. There were 280 trials, each lasting 9 seconds. Every trial begins with a fixed cross and a brief buzz. A visual cue popped up after a few seconds, and the subject had 6 seconds to imagine the appropriate hand movements. Between 0.5 and 30 Hz, a band pass filter was used. This is illustrated in Figure 4-1The data was collected from a female participant. The dataset properties are shown in Table 4-1

The second dataset we used in this research is BCI Competition IV dataset 2b. EEG data is assembled from 9 subjects, where each subject had a total of five sessions. The first two sessions were taped without feedback, whereas the remaining three were taped with feedback. In this study data without feedback is used as dataset. In initial two sessions, each trial begins by a brief buzz and fixed cross. An arrows represent the Motor Imagery task at t = 3s. For 1.25 seconds, the arrow is perceptible. After that, the subjects have four seconds to imagine the task. Figure 4-2 depicts this procedure.

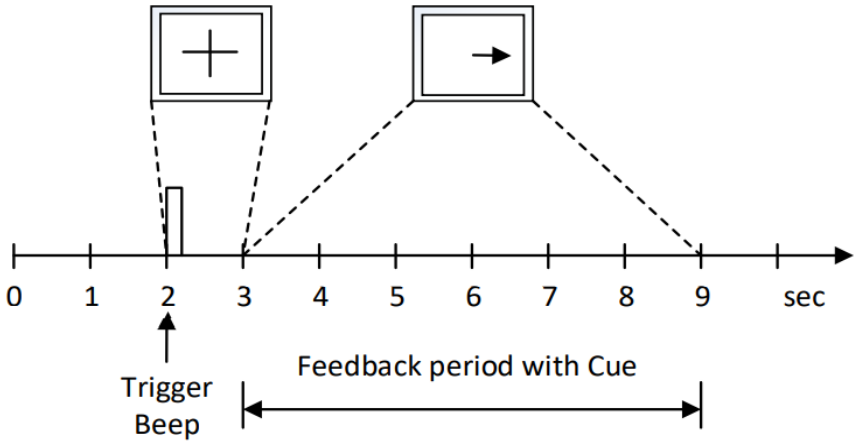

Figure 4-1: Paradigm used for the dataset III experiment

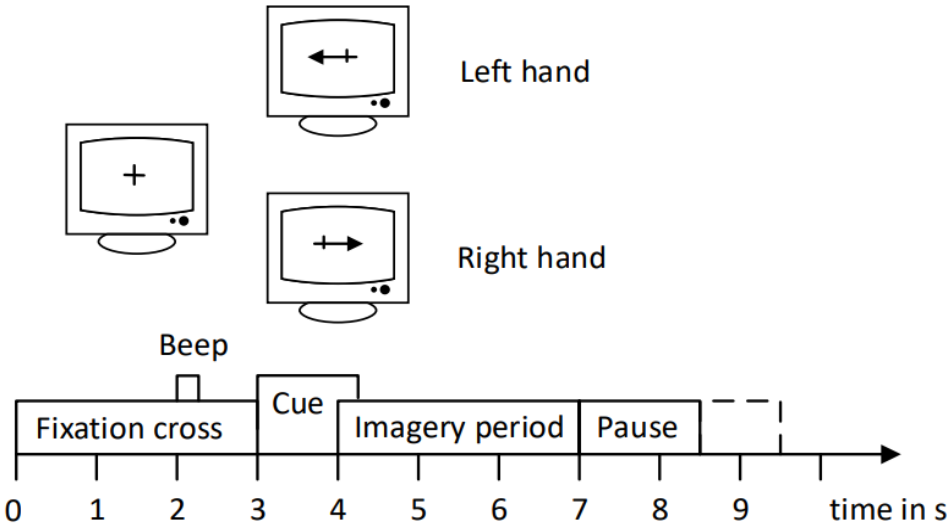

Figure 4-2: Paradigm used for the dataset IV2b experiment

Table 4-2 Dataset Properties

Dataset	Channels	Subjects	Sampling Frequency	Trails
Dataset III from BCI Competition II	C3, C z, C4	1	128	280
Dataset 2b from Competition IV	C3, C z, C4	9	250	400

4.2 Results

The training set of dataset 2b from BCI Competition IV [54] and dataset III from BCI Competition II [53] are employed to screen our approach. Our framework was assessed by two parameters, which are accuracy rate (%) and kappa coefficients. Measure of classification accuracy is also known as kappa coefficient. Kappa Coefficient is defined as

$$\boldsymbol{kappa} = \frac{\boldsymbol{accuracy - rand}}{\boldsymbol{1 - rand}} \qquad 12$$

Where rand is random classification accuracy which is taken as 0.5 [55].

In BCI Competition IV dataset 2b, the model was tested for each person independently. The model's accuracy and mean kappa value were investigated using K-fold cross validation [56]. When the training set is insufficient, loop estimation gathers as much data as possible, preventing the model from over-fitting. In this study, we used K = 5 to validate, and the outcome is calculated as the mean of the outcomes of these five models. Our results are then compared to other cutting-edge algorithms. **Table 4-3** displays our experimental results in the form of accuracy. **Table 4-3** shows our results in terms of kappa value.

We also compared our proposed model with our CNN and CNN-SAE architecture. The average accuracy of CNN, CNN-SAE, CNN-LSTM are 77.2%, 75.1% and 86.83% respectively. It is seen that CNN-LSTM perform better than CNN and CNN-SAE frameworks. We have also compared the results in the form of accuracy and kappa value, which are as shown in **Table 4-4** and **Table 4-5**

Table 4-4: Comparison with other methods in terms of accuracy.

	Accuracy(%)			
Subjects	**CNN [14]**	**IS-CBAM-CNN [18]**	**CNN-SAE [16]**	**CNN-LSTM** **Proposed Method**
1	85.71	80.3 ± 1.5	76.0 ± 2.7	91.4
2	78.57	75.0 ± 1.8	65.8 ± 1.9	83.1
3	92.15	67.7 ± 2.6	75.3 ± 1.8	84.6
4	95.67	95.4 ± 0.6	95.3 ± 0.4	82.1
5	89.20	88.3 ± 1.5	83.0 ± 1.4	79.3
6	85.12	80.0 ± 1.7	79.5 ± 2.5	89.2
7	79.23	73.7 ± 2.2	74.5 ± 1.8	93.4
8	81.28	77.4 ± 2.0	75.3 ± 2.6	89.5
9	80.67	78.6 ± 2.1	73.3 ± 3.6	88.9
Average	85.59	79.6 ± 1.8	77.6 ± 2.1	86.83

Table 4-5: Comparison with other methods in terms of kappa value.

Kappa value				
Subjects	**Twin SVM [58]**	**IS-CBAM-CNN [18]**	**CNN-SAE [16]**	**CNN- LSTM Proposed Method**
1	0.494	0.606 ± 0.030	0.517 ± 0.095	0.88
2	0.416	0.500 ± 0.036	0.324 ± 0.065	0.662
3	0.322	0.354 ± 0.052	0.494 ± 0.084	0.692
4	0.897	0.908 ± 0.012	0.905 ± 0.017	0.642
5	0.722	0.766 ± 0.030	0.655 ± 0.060	0.586
6	0.405	0.600 ± 0.034	0.579 ± 0.099	0.784
7	0.466	0.474 ± 0.044	0.488 ± 0.065	0.868
8	0.477	0.548 ± 0.040	0.494 ± 0.106	0.79
9	0.503	0.572 ± 0.042	0.463 ± 0.152	0.778
Average	0.526	0.592 ± 0.036	0.547 ± 0.083	0.742

Table 4-6: Comparison with CNN, CNN-LSTM in terms of accuracy

Subjects	CNN	CNN-LSTM
1	78.1	91.4
2	71.3	83.1
3	62.3	84.6
4	91.8	82.1
5	81.2	79.3
6	76.8	89.2
7	72.1	93.4
8	77.3	89.5
9	84.5	88.9
Average	77.2	86.83

Table 4-5: Comparison with CNN, CNN-LSTM in terms of kappa value

Subjects	CNN	CNN-LSTM
1	0.562	0.88
2	0.426	0.662
3	0.246	0.692
4	0.836	0.642
5	0.624	0.586
6	0.536	0.784
7	0.442	0.868
8	0.546	0.79
9	0.69	0.778
Average	0.545	0.742

We evaluated our model on another data i.e. dataset III from BCI Competition II. To determine classification efficiency, we used K-fold cross-validation. We gained 96.43% classification accuracy and a kappa value 0.9286 is obtained. The final results are then compared to other cutting-edge algorithms. Comparison is shown in Table6.

In this study, we also compared our model with the results with our CNN and CNN-SAE architecture. The average accuracy of CNN, CNN-SAE, CNN-LSTM are 88.1%, 92.1%, 96.43 %. We also compared in terms of kappa value. **Table 4-6, Table 4-7** show the comparison results.

Table 4-6: Comparison with other methods

Method	**[57]**	**CNN-SAE [16]**	**IS-CBAM-CNN [18]**	**CNN-LSTM Proposed Method**
Accuracy(%)	88.2	90.0	90.7	96.43
kappa	0.764	0.800	0.814	0.9286

Table 4-7: Comparison with CNN, CNN-SAE, CNN-LSTM methods

Method	**CNN**	**CNN-SAE**	**CNN-LSTM**
Accuracy(%)	88.1	92.1	96.43
kappa	0.762	0.842	0.9286

CHAPTER 5: CONCLUSION

5.1 Conclusion

This study proposed, a combined form of Convolutional Neural Network and LSTM for features extraction as well as for classification. The CNN Architecture consists of four blocks for features extraction. Each block is composed of the following layers: a convolutional layer, a batch normalization layer, a RELU activation layer, and then a max-pooling layer. On the BCI competition II dataset III, the proposed model is trained and evaluated. The wavelet transform is employed in the proposed method to transform a 1D signal to a 2D image. The wavelet transform was chosen because of its ability to analyze data at multiple scales. A CNN is employed to extract robust features from images, and then the EEG signals are classified using LSTM. Experiments show that integrating CNN and LSTM networks outperforms traditional methods. Our proposed method is the most accurate, with a 96.1 % accuracy.

5.2 Future Work

We summaries some of the prospective study directions in the following section:

Multi-class BCIs: Frameworks for multi-class BCIs can be developed.

Overfitting: We will try to reduce Overfitting. Overfitting occurs in our model due to noise. We will try to reduce overfitting in future and try to improve classification accuracy.

Advanced Classification Models: More advanced categorization models will be tested.

BIBLIOGRAPHY

[1] Padfield N, Zabalza J, Zhao H, Masero V and Ren J 2019 EEG-based brain-computer interfaces using motor-imagery: Techniques and challenges Sensors 19 1423

[2] Nicolas-Alonso L F and Gomez-Gil J 2012 Brain Computer Interfaces, a review *Sensors* **12** 1211–79

[3] Pfurtscheller G and Lopes da Silva F H 1999 Event-related EEG/MEG synchronization and desynchronization: Basic principles *Clinical Neurophysiology* **110** 1842–57

[4] Tang Z, Sun S, Zhang S, Chen Y, Li C and Chen S 2016 A brain-machine interface based on ERD/ERS for an upper-limb exoskeleton control *Sensors* **16** 2050

[5] Ahmed M, Shill P C, Islam K, Mollah M A and Akhand M A 2015 Acoustic modeling using Deep Belief Network for bangla speech recognition *2015 18th International Conference on Computer and Information Technology (ICCIT)*

[6] Dobhal T, Shitole V, Thomas G and Navada G 2015 Human activity recognition using binary motion image and Deep Learning *Procedia Computer Science* **58** 178–85

[7] Mikolov T, Deoras A, Kombrink S, Burget L and Černocký J 2011 Empirical evaluation and combination of advanced language modeling techniques *Interspeech 2011*

[8] Kumar S, Sharma A, Mamun K and Tsunoda T 2016 A deep learning approach for motor imagery EEG Signal Classification *2016 3rd Asia-Pacific World Congress on Computer Science and Engineering (APWC on CSE)*

[9] Zheng W-L, Zhu J-Y, Peng Y and Lu B-L 2014 EEG-based emotion classification using Deep Belief Networks *2014 IEEE International Conference on Multimedia and Expo (ICME)*

[10] You Y, Chen W and Zhang T 2020 Motor imagery EEG classification based on flexible analytic wavelet transform *Biomedical Signal Processing and Control* **62** 102069

[11] Xu B, Zhang L, Song A, Wu C, Li W, Zhang D, Xu G, Li H and Zeng H 2019 Wavelet transform time-frequency image and convolutional network-based motor imagery EEG classification *IEEE Access* **7** 6084–93

[12] Wang H and Bezerianos A 2017 Brain-controlled wheelchair controlled by sustained and brief motor imagery bcis *Electronics Letters* **53** 1178–80

[13] Graimann B, Allison B and Pfurtscheller G 2010 Brain-Computer Interfaces: Springer) pp 1-27

[14] Gray H and Lewis W H 2000 *Anatomy of the human body* (Bartleby.com)

[15] Futagi Y, Ishihara T, Tsuda K, Suzuki Y and Goto M 1998 Theta rhythms associated with sucking, crying, gazing and handling in infants *Electroencephalography and Clinical Neurophysiology* **106** 392–9

[16] Wolpaw J R and McFarland D J 2004 Control of a two-dimensional movement signal by a noninvasive brain-computer interface in humans *Proceedings of the National Academy of Sciences* **101** 17849–54

[17] Abo-Zahhad M, Ahmed S M and Abbas S N 2015 A new EEG acquisition protocol for biometric identification using eye blinking signals *International Journal of Intelligent Systems and Applications* **7** 48–54

[18] Tanner, A. et al. 2011. Automatic seizure detection using a two-dimensional eeg feature space. Master's thesis, Aalto University

[19] Pfurtscheller G and Neuper C 2001 Motor imagery and direct brain-computer communication *Proceedings of the IEEE* **89** 1123–34

[20] Szachewicz. A et al 2013. Classification of motor imagery for brain-computer interfaces, Poznan University of Technology Faculty of Computing and Information Science Institute of Computing Science

[21] Leila Azinfar Reza Fazel-Rezai Setare Amiri, Ahmed Rabbi. 2013. Brain-computer interface systems – recent progress and future prospects. In BCI Integration: Application Interfaces.

[22] Lin Z, Zhang C, Wu W and Gao X 2007 Frequency recognition based on canonical correlation analysis for SSVEP-based BCIs *IEEE Transactions on Biomedical Engineering* **54** 1172–6

[23] Hinterberger T, Schmidt S, Neumann N, Mellinger J, Blankertz B, Curio G and Birbaumer N 2004 Brain-computer communication and slow cortical potentials *IEEE Transactions on Biomedical Engineering* **51** 1011–8

[24] Birbaumer N, Ghanayim N, Hinterberger T, Iversen I, Kotchoubey B, Kübler A, Perelmouter J, Taub E and Flor H 1999 A spelling device for the Paralysed *Nature* **398** 297–8

[25] Rakotomamonjy A and Guigue V 1970 Figure 1 from BCI competition III: Dataset II-ensemble of svms for BCI p300 speller: Semantic scholar *undefined*

[26] Pfurtscheller G and Lopes da Silva F H 1999 Event-related EEG/MEG synchronization and desynchronization: Basic principles *Clinical Neurophysiology* **110** 1842–57

[27] Lemm S, Müller K-R and Curio G 2009 A generalized framework for quantifying the dynamics of EEG event-related desynchronization *PLoS Computational Biology* **5**

[28] Raudys S J and Jain A K 1991 Small sample size effects in statistical pattern recognition: Recommendations for practitioners *IEEE Transactions on Pattern Analysis and Machine Intelligence* **13** 252–64

[29] Tabar,Y et, A. et al. 2017. Motor Imagery EEG Signal Classification using Deep learning for Brain computer interfaces. Master's thesis, Middle East Technical University

[30] Sellers E W, Vaughan T M and Wolpaw J R 2010 A brain-computer interface for long-term independent home use Amyotrophic lateral sclerosis 11 449-55

[31] Farwell L A and Donchin E 1988 Talking off the top of your head: toward a mental prosthesis utilizing event-related brain potentials Electroencephalography and clinical Neurophysiology 70 510-23

[32] Townsend G, LaPallo B, Boulay C, Krusienski D, Frye G, Hauser C, Schwartz N, Vaughan T, Wolpaw J R and Sellers E 2010 A novel P300-based brain–computer interface stimulus presentation paradigm: moving beyond rows and columns Clinical Neurophysiology 121 1109-20

[33] Takano K, Komatsu T, Hata N, Nakajima Y and Kansaku K 2009 Visual stimuli for the P300 brain–computer interface: a comparison of white/gray and green/blue flicker matrices Clinical neurophysiology 120 1562-6

[34] Li Y, Nam C S, Shadden B B and Johnson S L 2010 A P300-based brain– computer interface: Effects of interface type and screen size Intl. Journal of Human–Computer Interaction 27 52-68

[35] Ahi S T, Kambara H and Koike Y 2011 A dictionary-driven P300 speller with a modified interface IEEE Transactions on Neural Systems and Rehabilitation Engineering 19 6-14

[36] Cheng M, Gao X, Gao S and Xu D 2002 Design and implementation of a brain-computer interface with high transfer rates IEEE transactions on biomedical engineering 49 1181-6

[37] Trejo L J, Rosipal R and Matthews B 2006 Brain-computer interfaces for 1- D and 2-D cursor control: designs using volitional control of the EEG spectrum or steady-state visual evoked potentials IEEE transactions on neural systems and rehabilitation engineering 14 225-9

[38] Allison B Z, McFarland D J, Schalk G, Zheng S D, Jackson M M and Wolpaw J R 2008 Towards an independent brain–computer interface using steady state visual evoked potentials Clinical neurophysiology 119 399-408

[39] Segers H, Combaz A, Manyakov N V, Chumerin N, Vanderperren K, Van Huffel S and Van Hulle M 2011 Steady state visual evoked potential (SSVEP)-based brain spelling system with synchronous and asynchronous typing modes. In: 15th Nordi.-Balt. Conf. Biomed. Eng. Med. Phys: Springer) pp 164-7

[40] Yin E, Zhou Z, Jiang J, Yu Y and Hu D 2015 A dynamically optimized SSVEP brain–computer interface (BCI) speller IEEE Transactions on Biomedical Engineering 62 1447-56

[41] Xu B, Zhang L, Song A, Wu C, Li W, Zhang D, Xu G, Li H and Zeng H 2019 Wavelet transform time-frequency image and convolutional network-based motor imagery EEG classification IEEE Access 7 6084–93

[42] Leeb R, Lee F, Keinrath C, Scherer R, Bischof H and Pfurtscheller G 2007 Brain–Computer Communication: Motivation, AIM, and impact of exploring a virtual apartment IEEE Transactions on Neural Systems and Rehabilitation Engineering 15 473–82

[43] Zhao J, Mao X and Chen L 2019 Speech emotion recognition using Deep 1D & 2D CNN LSTM Networks Biomedical Signal Processing and Control 47 312–23

[44] Y. Lecun, B.E. Boser, J.S. Denker, D. Henderson, R.E. Howard, W. Hubbard, L.D. Jackel, Backpropagation applied to handwritten zip code recognition, Neural Comput. 1 (4) (1989) 541–551.

[45] Boser B E, Sackinger E, Bromley J, LeCun Y, Howard R E and Jackel L D An analog neural network processor and its application to high-speed character recognition IJCNN-91-Seattle International Joint Conference on Neural Networks

[46] Behnke S, 2003 Discovering hierarchical speech features using convolutional non-negative matrix factorization Proceedings of the International Joint Conference on Neural Networks.

[47] Palaz D, Collobert R and Magimai-Doss M 2013 Estimating phoneme class conditional probabilities from raw speech signal using Convolutional Neural Networks *Interspeech*

[48] Z. C. Lipton, J. Berkowitz, and C. Elkan, 2015 “A critical review of recurrent neural networks for sequence learning,” arXiv preprint arXiv:1506.00019

[49] Zhang G, Davoodnia V, Sepas-Moghaddam A, Zhang Y and Etemad A 2020 Classification of hand movements from EEG using a deep attention-based LSTM network *IEEE Sensors Journal* **20** 3113–22

[50] Hochreiter S and Schmidhuber J 1997 Long short-term memory *Neural Computation* **9** 1735–80

[51] Gers F A, Schmidhuber J and Cummins F 2000 Learning to forget: Continual prediction with LSTM *Neural Computation* **12** 2451–71

[52] Rastogi M 2021 Tutorial on LSTM: A computational perspective *Medium*

[53] Schlögl A 2003 Outcome of the BCI-Competition 2003 on the Graz Data Set (Berlin: Graz University of Technology)

[54] Leeb R, Lee F, Keinrath C, Scherer R, Bischof H and Pfurtscheller G 2007 Brain–Computer Communication: Motivation, AIM, and impact of exploring a virtual apartment IEEE Transactions on Neural Systems and Rehabilitation Engineering 15 473–82

[55] Tabar Y R and Halici U 2016 A novel deep learning approach for classification of EEG motor imagery signals Journal of Neural Engineering 14 016003

[56] Xiao X and Fang Y 2021 Motor imagery EEG signal recognition using Deep Convolution Neural Network Frontiers in Neuroscience 15

[57] Ren Y and Wu Y 2014 Convolutional deep belief networks for feature extraction of EEG signal 2014 Int. Joint Conf. on Neural Networks (IJCNN) (IEEE) pp 2850–3

[58] Soman S 2015 High performance EEG signal classification using classifiability and the Twin SVM Appl. Soft Comput. 30 305–18

Completion Certificate

It is to certify that the thesis titled **Analysis and Classification of EEG Signals** submitted by Regn. No **00000319157**, NS **Muneeb Arshad** of MS-19 Electrical Engineering has been found satisfactory for the requirement of degree of Master of Science.

Thesis Supervisor:

_____

Dr. Shahzad Amin Sheikh